Rapid Communications | Editors' Suggestion

Ramsey fringes in a room-temperature quantum-dot semiconductor optical amplifier

I. Khanonkin,[1,2,*] A. K. Mishra,[1,2] O. Karni,[3] S. Banyoudeh,[4] F. Schnabel,[4] V. Sichkovskyi,[4] V. Mikhelashvili,[1,2] J. P. Reithmaier,[4] and G. Eisenstein[1,2]

[1]*Russell Berrie Nanotechnology Institute, Technion, Haifa 32000, Israel*

[2]*Andrew and Erna Viterbi Department of Electrical Engineering, Technion, Haifa 32000, Israel*

[3]*E. L. Ginzton Laboratory, Applied Physics Department, Stanford University, Stanford, California 94305, USA*

[4]*Institute of Nanostructure Technologies and Analytics, Technische Physik, CINSaT, University of Kassel, D-34132 Kassel, Germany*

(Received 5 December 2017; revised manuscript received 1 June 2018; published 26 June 2018)

The ability to induce, observe, and control quantum coherent interactions in room-temperature, electrically driven optoelectronic devices is of utmost significance for advancing quantum science and engineering towards practical applications. We demonstrate here a coherent interference phenomena, Ramsey fringes, in an inhomogeneously broadened InAs/InP quantum-dot (QD) ensemble in the form of a 1.5-mm-long optical amplifier operating at room temperature. The observation of Ramsey fringes in semiconductor QDs was previously achieved only at cryogenic temperatures and only in isolated single-dot systems. A high-resolution pump-probe scheme where both pulses are characterized by cross-frequency-resolved optical gating reveals a clear oscillatory behavior both in the amplitude and the instantaneous frequency of the probe pulse with a period that equals one optical cycle at the operational wavelength. Using nominal input delays of 600–900 fs and scanning the separation around each delay in 1-fs steps, we map the evolution of the material decoherence and extract a coherence time of 340 fs. Moreover, we observed a unique phenomenon, which cannot be observed in single-dot systems, that the temporal position of the output probe pulse also oscillates with the same periodicity but with a quarter cycle delay relative to the intensity variations. The modulation of the pulse separation results from coupling between the real and imaginary parts of the susceptibility and the quadrature delay is the time domain manifestation of its complex nature.

DOI: 10.1103/PhysRevB.97.241117

Semiconductor quantum dots (QDs) serve routinely as a viable platform for basic quantum mechanical experiments and detailed understanding of light-matter interactions [1,2]. The use of QDs for quantum applications such as generation of single photons [3–6] and entangled photon pairs [7–10], photon-echo-based quantum memories [11], and quantum gates [12] have been demonstrated often and are well documented.

The basic quantum mechanical phenomena, e.g., Rabi oscillation [13], Ramsey interference [14], etc., enable control over final quantum states. Unlike Rabi oscillation, Ramsey interference involves two time-delayed pulses and hence it requires substantially better control over the coherent evolution of the quantum state [14]. An early measurement of Ramsey fringes in a single GaAs QD, which was formed by width fluctuations of a quantum well, was observed using photoluminescence (PL) measurements by Bonadeo [15]. Similar Ramsey-type oscillations in a single InGaAs QD selected from a low-density self-assembled system was reported by Toda [16] and Htoon [17]. Photocurrent measurements in electric-field-tunable single QD systems were used to demonstrate Ramsey interference by Stufler [18] and by Michaelis [19]. Two- and three-pulse photon-echo experiments also enabled the observation of Ramsey fringes in a single InAs/GaAs QD, as reported by Jayakumar [20]. A different aspect of Ramsey interference addressed the spin state of QD which was interrogated using ultrafast optical techniques by Press [21], by Kim [22], and by Lagoudakis [23]. Common to all these reports is the fact that only isolated single quantum dots, held at cryogenic temperatures, were used.

Another class of quantum coherent experiments in semiconductor media was reported by Choi [24], who showed Rabi oscillations in a quantum cascade semiconductor laser. Coherent light-matter interactions in QD ensembles were studied by Marcinkevicius [25], who demonstrated electromagnetic-induced transparency in a stack of InGaAs/GaS QDs, and by Suzuki [26], who used two-dimensional coherent spectroscopy to study an ensemble of InAs/GaAs QDs. Those experiments were also performed at cryogenic temperatures.

We use a different approach to induce and observe coherent phenomena in QD systems in which ultrashort optical pulses excite a QD ensemble operating at room temperature. The platform we employ is an electrically driven QD-based semiconductor optical amplifier (QD SOA), which is a long waveguide that provides optical gain. Such experiments have to overcome several hurdles. One is the short room-temperature coherence time which was previously determined from the temperature-dependent PL linewidth of a single QD by Bayer [27] to be 300 fs. Transient four-wave mixing measured in a GaAs QD SOA by Borri [28] found a bias-dependent coherence time ranging from 250 at zero bias to 50 fs at 20 mA when the amplifier approaches transparency or low gain. The bias dependence of the coherence time is consistent with the findings in Ref. [29]. Other difficulties stem from

*ikhanonkin@technion.ac.il

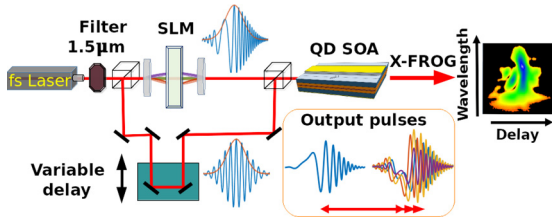

FIG. 1. Schematic diagram of the pump-probe X-FROG system. A 150-fs-wide pump pulse is shaped by an SLM in order to prevent input pulse overlap and to enhance the induction of a coherent state to be sensed by the probe.

the QD ensemble inhomogeneity and the fact that incoherent interactions such as two-photon absorption, and an associated Kerr-like effect, take place simultaneously and can mask coherent interactions. Nevertheless, using 150-fs single excitation pulses, Rabi oscillations were demonstrated by Karni in an InAs/InP QD [30] and by Capua in InAs/InP quantum dash (wirelike nanostructures) [31] SOAs employing the cross-frequency-resolved optical gating (X-FROG) technique and later by Kolarczik in an InAs/GaAs QD SOA [32] using a technique called FROSCH (frequency-resolved optical short-pulse characterization by heterodyning). The role of the gain inhomogeneity and the incoherent interactions was considered by Karni [33], as was a demonstration of coherent control to enhance the Rabi oscillations by using shaped excitation pulses [34]. A different type of coherent control with a two-pulse pump-probe X-FROG was used by Capua [35] to demonstrate cyclical instantaneous frequency variation of the probe pulse in a QD SOA that was biased to the absorption regime. No trace of a periodic intensity oscillation was observed in that experiment, probably because of a severe dot inhomogeneity (the PL linewidth for a single QD layer was 31 meV, almost twice that of the present QD material [36]). Also, the low signal-to-noise ratio (stemming from the large absorption) requires one to operate far from the absorption peak where the interaction of the electromagnetic field with the QDs was significantly reduced.

We report here an observation of Ramsey fringes in a room temperature, inhomogeneously broadened ensemble of QDs. Measuring Ramsey fringes requires a significantly more intricate experimental procedure as compared to single-pulse experiments which reveal Rabi oscillations, since it requires careful control over two pulses and their temporal separation. A series of experiments we performed using a pump-probe X-FROG system that includes shaping of the pump pulse demonstrate a clear oscillatory behavior, with a period equal to an optical cycle, of both the intensity and the instantaneous frequency profiles of the probe pulse. The oscillation modulation depth decreases with a nominal input pulse delay, thereby enabling direct mapping of the decoherence.

An additional major finding described in this Rapid Communication is an oscillation of the output temporal pulse separation caused by the coupling between the real and imaginary parts of the material susceptibility. The experimental results were confirmed by a previously reported comprehensive numerical model [34,37].

The experimental setup is shown schematically in Fig. 1. A fiber laser (Toptica FemtoFiber pro) generated pulses at a repetition rate of 40 MHz which are filtered to obtain 150-fs pulses centered at 1.55 μm. The pulses are split with one arm traversing a liquid-crystal-based spatial light modulator (SLM) (Jenoptiks SLM-S640 with a broadband antireflective coating) and the other passing through a highly accurate motorized delay line, the resolution of which is better than 1 fs.

The two pulses are recombined before they are coupled into a QD SOA. The SLM is used to adjust the spectral phase of the pump pulse in order to remove a moderate trailing edge wing of the pulse and prevent any overlap of the input pulses. In Ref. [34] it was shown that positively chirped excitations enhance Rabi oscillations when the pulse is spectrally placed on the short-wavelength side of the gain spectrum. Negatively chirped pulses do the same for pulses place on the long-wavelength side. In the present case, the input pulses matched the gain peak but redshifted somewhat upon propagation. Therefore, we induced a negative chirp on the input pulses to ensure an optimized interaction [34]. The input energies of the pump and probe pulses are 35 and 20 pJ, respectively. The pulses are measured at the SOA output using the X-FROG technique [38]. The amplitude and phase profiles are obtained from the measured data using a phase retrieval algorithm [38] with a convergence error below 1%.

QD-based SOA operates at 1.55-μm wavelength and comprises six InAs dot layers grown by molecular beam epitaxy in the Stranski-Krastanov growth mode [39]. Each layer has a density of about 6×10^{10} cm^{-2} with a record uniformity characterized by a photoluminescence linewidth of 17 meV at 10 K [40]. Layer stacking broadens the linewidth due to strain-related inhomogeneities. The linewidth of the six-layer structure is nevertheless very narrow, 30 meV [36]. The emission level of electroluminescence spectra increases with bias but the spectral shape remains unchanged [41]; no blueshift due to the plasma effect or a redshift due to self-heating take place. This signifies that the QDs do not saturate and the maximum possible gain is obtainable for each drive current. The large density and the dot uniformity yield a large modal gain of 15 cm^{-1} per dot layer which enables superb laser characteristics [42]. The optical amplifier was realized by coating the end facets of a 1.5-mm-long, 2-μm-wide ridge laser with a two-layer dielectric antireflection coating yielding a modal reflectivity of 0.01%. In the experiments described hereon, the amplifier was biased at 210 mA, corresponding to a current density of 7 kA cm^{-2}, where it exhibits a large gain of 30 dB. The coherent interactions depend on the pulse area. Therefore, a lower gain can be compensated for, in principle, by using more energetic pulses.

The intensity and instantaneous frequency profiles of the output pulses for temporal delays of 600–612 fs are shown in Fig. 2. The profiles of the pump pulse are naturally independent of the delay, however, the probe pulse exhibits cyclical intensity variations accompanied by oscillations in the instantaneous frequency profile. The pump pulse sets a coherent state for each QD emitter whose transition energy overlaps the pump pulse spectrum, which is sensed by the probe pulse whose phase, relative to that of the coherent state, varies as the delay changes in 1-fs steps (which corresponds to less than a quarter of an optical cycle), resulting in the oscillatory behavior which is a clear indication of Ramsey interference fringes [43].

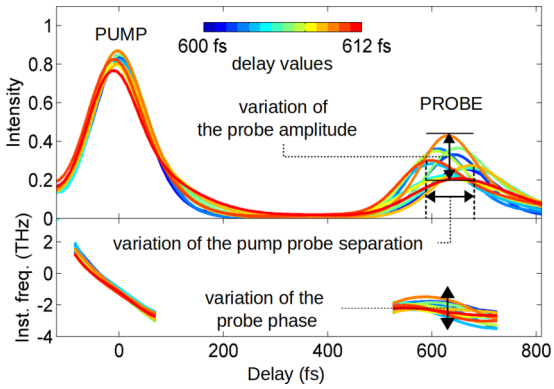

FIG. 2. X-FROG traces of the two pulses for a nominal delay of 600 fs. The upper trace shows intensity profiles for delays of 600–612 fs. The lower trace shows the corresponding instantaneous frequencies. The pump pulse is delay independent but the probe pulse exhibits clear Ramsey fringes with a periodicity of one optical cycle, ~5fs.

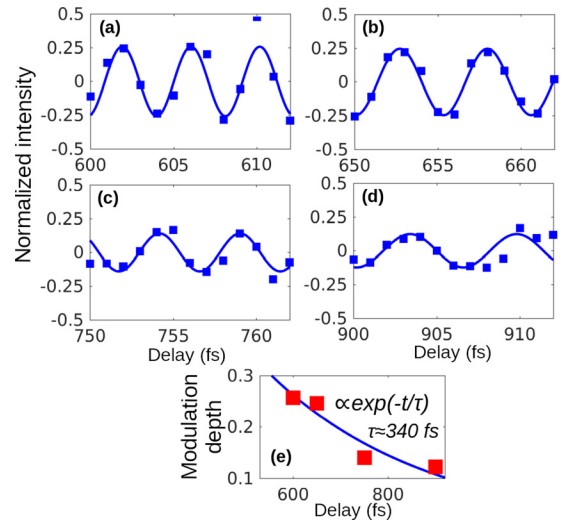

FIG. 4. Normalized intensities of the probe pulse for various nominal delays: (a) 600, (b) 650, (c) 750, (d) 900 fs. Each figure represents a 12-fs delay span. The decay of the modulation depth with nominal delay is clearly seen. It represents a direct mapping of the loss of coherence. (e) Modulation depth (squares) as a function of nominal delay from which a coherence time of 340 fs is extracted by a fit (solid line) to an exponential function.

The evolution of the probe pulse intensity and its instantaneous frequency profiles are shown in Fig. 3. The intensity oscillates with a period of roughly 5 fs and the modulation depth is 50%. The instantaneous frequency profile is also cyclical with the same periodicity.

The dependence of the probe intensity oscillations on nominal input delay is described in Figs. 4(a)–4(d), which show the normalized intensity of the probe pulse for four sets of delays: 600, 650, 750, and 900 fs. The aforementioned normalization was processed for measured intensities y as $\frac{y}{\frac{y_{max}+y_{min}}{2}} - 1$, where y_{min} and y_{max} are minimal and maximal values of the peak pulse intensity variations. An input delay of 600 fs is the shortest separation for which there is absolutely no input pulse overlap. This ensures that no interference occurs, which can mask the QD-mediated coherent coupling between the pulses.

The period of the amplitude oscillations in the set of nominal delays, 600–900 fs, varies slightly around 5 fs. According to Salour [43], the period of oscillations depends on the detuning between the QDs transition frequency and the input pulses. The deviations from 5 fs might originate from nonresonant effects that take place simultaneously with the coherent interaction. Nonlinear incoherent propagation effects can shift the carrier wavelength and hence the detuning from the transition energy. Also, a comprehensive model for the dynamics of a QD laser [44] shows that an internal field established by a Coulomb interaction between electrons and holes modifies the energy bands. This may result in a Stark shift which also changes the detuning. The pump pulse always interacts with the same material state. The probe pulse, however, interacts with a material that recovers from the modifications induced by the pump pulse. This means that for different nominal delays, the effects of nonlinear propagation and internal Coulomb fields

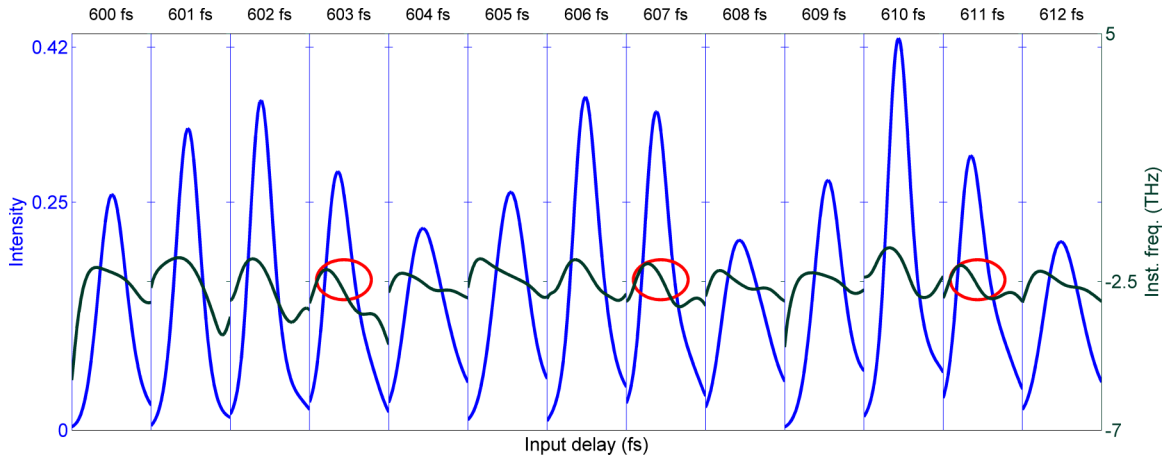

FIG. 3. Measured Ramsey fringes. Measurements of intensity (blue traces) and instantaneous frequency (green traces) profiles for a delay range of 600–612 fs. The intensity and instantaneous frequency are cyclical with a period of an optical cycle at 1.55 μm (~5fs). The instances when the instantaneous frequency repeats itself are marked by red circles.

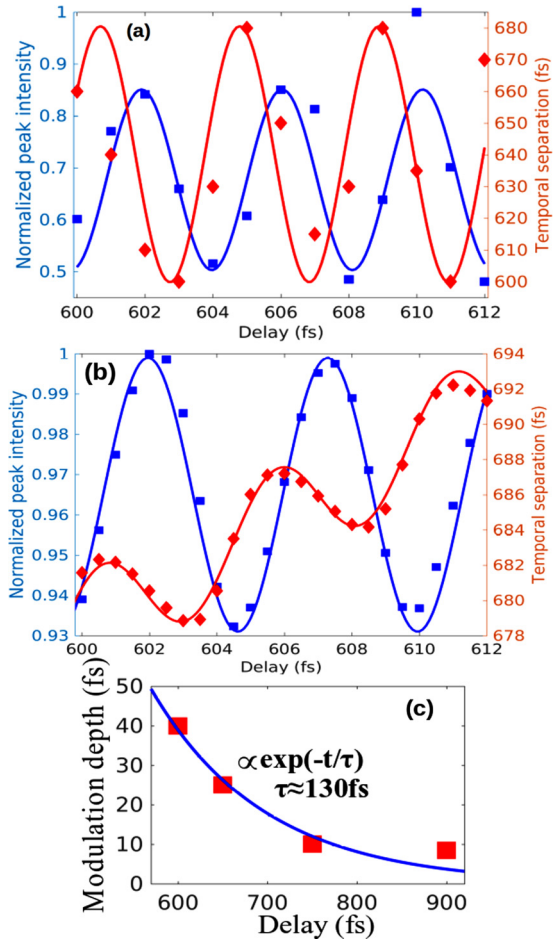

FIG. 5. Normalized intensity and output pulse separation for a delay range of 600–612 fs. (a) Measured, in steps of 1 fs, amplitude variations (blue trace) and output pulse separations (red trace). (b) Simulated results, shown in steps of 0.5 fs, confirming the measurements shown in (a). The variation of the output pulse separation lags behind the intensity modulation by a quarter of a cycle (around 1 fs) due to the complex nature of the susceptibility. (c) Measured output separation as a function of nominal input delay. An exponential fit yields a decay with a time constant of 130 fs.

have a different impact and hence may change the detuning. The periodicity changes due to detuning were observed in Ref. [18], where an intentional detuning induced by the Stark shift was used to control the periodicity of Ramsey fringes. The slight changes in periodicity are related to the detuning, but this by itself cannot explain the entire change. We postulate therefore that a system instability also plays a role in the observed variation in periodicity.

The intensity modulation depths are summarized in Fig. 4(e), which represents a direct mapping of the loss of coherence. A fit to an exponential decay (with an error of $R^2 \sim 0.9$) yields an extracted room-temperature coherence time of 340 fs.

The amplitude oscillations of the probe pulse are accompanied by a unique phenomenon—an oscillation in the output pulse temporal separation. The amplitude changes cause modifications of the carrier density which modulates, in turn, the real part of the susceptibility and hence the group velocity and the pulse propagation time. This coupling is due to the well-known Henry α parameter, which is defined as the ratio between the derivatives, with respect to carrier density, of the real and imaginary parts of the susceptibility [45]. This is shown in Fig. 5(a) for delays of 600–612 fs, where the measured peak output intensity of the probe pulse is plotted as a blue trace and the output temporal separation between the peaks of the output pulses is shown in the red trace. Both exhibit a Ramsey-type fringe pattern with the same oscillation frequency but with a quarter cycle phase shift. The phase shift stems from the fact that changes in the real part of the susceptibility, induced by modulation of the imaginary part, translate in the time domain to a delay of a quarter of a cycle. The maximum temporal separation between output pump and probe pulses is 80 fs at a delay of 600 fs. This can be translated to a relative change of the effective refractive index, of $\frac{\Delta n}{n} \approx 5 \times 10^{-3}$. This reduces at 900 fs to less than 20 fs or $\frac{\Delta n}{n} \approx 1.25 \times 10^{-3}$.

A comprehensive finite-difference time domain model was used to simulate the observed Ramsey fringes with the measured input pulses used as the excitation. The model treats the active medium of the amplifier as a cascade of effective two-level systems [37]. It calculates the coevolution of the electromagnetic wave and the electronic state of the gain medium along the propagation axis of the amplifier by solving simultaneously Maxwell's and Schrödinger equations in the density matrix formalism. The model accounts also for the QD gain inhomogeneity as well as for nonresonant propagation effects [33]. The simulation results are shown in Fig. 5(b). Both the pump and probe at the input are negatively chirped, 150-fs-wide Gaussian pulses. The oscillations of the peak intensity as well as the pulse separation resemble the measured results. The phase shift between the amplitude and temporal separation oscillation is one quarter cycle in both experiment and simulation. The amplitude of the temporal changes is lower in the simulation as compared to the experiment. This discrepancy results from some unknown material parameters that affect the simulated results and complex input experimental pulse shapes that are not considered in the simulations. As the nominal delay increases, the Ramsey fringes in the temporal pulse separation are superimposed on the linear curve, which directly maps the increase of the input pump-probe delay. In the experiment, the linear part is masked due to a limited sensitivity of the detection system.

The dependence on a nominal delay of the output pulse separation [Fig. 5(a)] follows a similar trend to that of the amplitude modulation depth, namely, it decays exponentially with a time constant of 130 fs as the delay increases, as shown in Fig. 5(c). This value differs from that in Fig. 4(e) due to two main reasons. First, the intensity is determined by the optical gain which is nonlinear, $G \sim \exp(gL)$, where G is the total gain, g is the gain coefficient (which is determined by the carrier density), and L is the SOA length. On the other hand, the change of separation is linearly proportional to the change in carrier density through the real part of the optical susceptibility. Second, the α parameter is itself nonlinear in a QD gain medium [46].

To conclude, we have used a high-resolution two-pulse pump-probe X-FROG system to demonstrate Ramsey interference in an electrically driven 1.55-μm InAs/InP QD SOA operating at room temperature. The probe intensity and its

instantaneous frequency profiles exhibit a cyclical behavior with a periodicity of about 5 fs, which equals a single optical cycle at 1.55 μm. The modulation depth in the oscillating probe intensity decreases with increasing nominal input delay and this enables a direct mapping of the decoherence process that the active gain medium undergoes and the extraction of a coherence time, which is found to be 340 fs. Above and beyond this, we also demonstrated a unique property by which the output separation between the two pulses also oscillates with the same periodicity and exhibits a delay of one quarter of a cycle relative to the intensity oscillation. The oscillations stem from coupling between the two parts of the susceptibility while the quarter cycle delay is a time domain manifestation of its complex nature. The oscillation in pulse separation is only possible in a distributed medium such as the QD SOA and cannot occur in the single QD systems used in many Ramsey interference experiments. The experimental results were confirmed by a comprehensive numerical model.

This work was funded by the Israel Science Foundation (1504/16). I.K. acknowledges Dr. Elena Khanonkin, Ori Eyal, and Shai Tsesses for help in performing the measurements. A.K.M. acknowledges support in part by the Technion and by Israel Council for Higher Education.

[1] J. P. Reithmaier, G. Sek, A. Loffler, C. Hofmann, S. Kuhn, S. Reitzenstein, L. V. Keldysh, V. Kulakovskii, T. Reinecke, and A. Forchel, Nature (London) **432**, 197 (2004).
[2] J. P. Reithmaier, Semicond. Sci. Technol. **23**, 123001 (2008).
[3] P. Michler, A. Kiraz, C. Becher, W. V. Schoenfeld, P. M. Petroff, L. Zhang, E. Hu, and A. Imamoglu, Science **290**, 2282 (2000).
[4] D. V. Regelman, U. Mizrahi, D. Gershoni, E. Ehrenfreund, W. V. Schoenfeld, and P. M. Petroff, Phys. Rev. Lett. **87**, 257401 (2001).
[5] J. Claudon, J. Bleuse, N. S. Malik, M. Bazin, P. Jaffrennou, N. Gregersen, C. Sauvan, P. Lalanne, and J.-M. Gérard, Nat. Photonics **4**, 174 (2010).
[6] M. Benyoucef, M. Yacob, J. Reithmaier, J. Kettler, and P. Michler, Appl. Phys. Lett. **103**, 162101 (2013).
[7] O. Benson, C. Santori, M. Pelton, and Y. Yamamoto, Phys. Rev. Lett. **84**, 2513 (2000).
[8] N. Akopian, N. H. Lindner, E. Poem, Y. Berlatzky, J. Avron, D. Gershoni, B. D. Gerardot, and P. M. Petroff, Phys. Rev. Lett. **96**, 130501 (2006).
[9] I. Schwartz, D. Cogan, E. R. Schmidgall, Y. Don, L. Gantz, O. Kenneth, N. H. Lindner, and D. Gershoni, Science **354**, 434 (2016).
[10] R. J. Young, R. M. Stevenson, P. Atkinson, K. Cooper, D. A. Ritchie, and A. J. Shields, New J. Phys. **8**, 29 (2006).
[11] S. Poltavtsev, M. Salewski, Y. V. Kapitonov, I. Yugova, I. Akimov, C. Schneider, M. Kamp, S. Höfling, D. Yakovlev, A. Kavokin *et al.*, Phys. Rev. B **93**, 121304 (2016).
[12] G. Burkard, D. Loss, and D. P. DiVincenzo, Phys. Rev. B **59**, 2070 (1999).
[13] I. I. Rabi, S. Millman, P. Kusch, and J. R. Zacharias, Phys. Rev. **55**, 526 (1939).
[14] N. F. Ramsey, Rev. Mod. Phys. **62**, 541 (1990).
[15] N. H. Bonadeo, J. Erland, D. Gammon, D. Park, D. S. Katzer, and D. G. Steel, Science **282**, 1473 (1998).
[16] Y. Toda, T. Sugimoto, M. Nishioka, and Y. Arakawa, Appl. Phys. Lett. **76**, 3887 (2000).
[17] H. Htoon, T. Takagahara, D. Kulik, O. Baklenov, A. L. Holmes, Jr., and C. K. Shih, Phys. Rev. Lett. **88**, 087401 (2002).
[18] S. Stufler, P. Ester, A. Zrenner, and M. Bichler, Phys. Rev. Lett. **96**, 037402 (2006).
[19] S. M. De Vasconcellos, S. Gordon, M. Bichler, T. Meier, and A. Zrenner, Nat. Photonics **4**, 545 (2010).
[20] H. Jayakumar, A. Predojević, T. Huber, T. Kauten, G. S. Solomon, and G. Weihs, Phys. Rev. Lett. **110**, 135505 (2013).
[21] D. Press, T. D. Ladd, B. Zhang, and Y. Yamamoto, Nature (London) **456**, 218 (2008).
[22] D. Kim, S. G. Carter, A. Greilich, A. Bracker, and D. Gammon, Nat. Phys. **7**, 223 (2010).
[23] K. Lagoudakis, P. McMahon, C. Dory, K. Fischer, K. Müller, V. Borish, D. Dalacu, P. Poole, M. Reimer, V. Zwiller *et al.*, Optica **3**, 1430 (2016).
[24] H. Choi, V.-M. Gkortsas, L. Diehl, D. Bour, S. Corzine, J. Zhu, G. Höfler, F. Capasso, F. X. Kärtner, and T. B. Norris, Nat. Photonics **4**, 706 (2010).
[25] S. Marcinkevičius, A. Gushterov, and J. Reithmaier, Appl. Phys. Lett. **92**, 041113 (2008).
[26] T. Suzuki, R. Singh, M. Bayer, A. Ludwig, A. D. Wieck, and S. T. Cundiff, Phys. Rev. Lett. **117**, 157402 (2016).
[27] M. Bayer and A. Forchel, Phys. Rev. B **65**, 041308 (2002).
[28] P. Borri, W. Langbein, J. M. Hvam, F. Heinrichsdorff, M.-H. Mao, and D. Bimberg, Appl. Phys. Lett. **76**, 1380 (2000).
[29] M. Lorke, J. Seebeck, T. R. Nielsen, P. Gartner, and F. Jahnke, Phys. Status Solidi C **3**, 2393 (2006).
[30] O. Karni, A. Capua, G. Eisenstein, V. Sichkovskyi, V. Ivanov, and J. P. Reithmaier, Opt. Express **21**, 26786 (2013).
[31] A. Capua, O. Karni, G. Eisenstein, and J. P. Reithmaier, Phys. Rev. B **90**, 045305 (2014).
[32] M. Kolarczik, N. Owschimikow, J. Korn, B. Lingnau, Y. Kaptan, D. Bimberg, E. Schöll, K. Lüdge, and U. Woggon, Nat. Commun. **4**, 2953 (2013).
[33] O. Karni, A. K. Mishra, G. Eisenstein, and J. P. Reithmaier, Phys. Rev. B **91**, 115304 (2015).
[34] O. Karni, A. K. Mishra, G. Eisenstein, V. Ivanov, and J. P. Reithmaier, Optica **3**, 570 (2016).
[35] A. Capua, O. Karni, G. Eisenstein, V. Sichkovskyi, V. Ivanov, and J. P. Reithmaier, Nat. Commun. **5**, 1 (2014).
[36] S. Banyoudeh, A. Abdollahinia, V. Sichkovskyi, and J. Reithmaier, Proc. SPIE **9767**, 97670I (2016).
[37] A. Capua, O. Karni, and G. Eisenstein, IEEE J. Sel. Top. Quantum Electron. **19**, 1 (2013).
[38] R. Trebino, *Frequency-Resolved Optical Gating: The Measurement of Ultrashort Laser Pulses* (Springer, Berlin, 2012).
[39] C. Gilfert, E.-M. Pavelescu, and J. Reithmaier, Appl. Phys. Lett. **96**, 191903 (2010).
[40] S. Banyoudeh and J. P. Reithmaier, J. Cryst. Growth **425**, 299 (2015).

[41] I. Khanonkin, A. Mishra, O. Karni, V. Mikhelashvili, S. Banyoudeh, F. Schnabel, V. Sichkovskyi, J. Reithmaier, and G. Eisenstein, AIP Adv. **7**, 035122 (2017).

[42] S. Banyoudeh, A. Abdollahinia, O. Eyal, F. Schnabel, V. Sichkovskyi, G. Eisenstein, and J. P. Reithmaier, IEEE Photonics Technol. Lett. **28**, 2451 (2016).

[43] M. Salour, Rev. Mod. Phys. **50**, 667 (1978).

[44] D. Gready and G. Eisenstein, IEEE J. Sel. Top. Quantum Electron. **19**, 1900307 (2013).

[45] C. Henry, IEEE J. Quantum Electron. **18**, 259 (1982).

[46] B. Lingnau, K. Lüdge, W. W. Chow, and E. Schöll, Phys. Rev. E **86**, 065201 (2012).